Astronomy & Astrophysics manuscript no. main
July 9, 2025

Can dynamic dark energy explain the S_8 tension, the 'lensing is low' effect, or strong baryon feedback?

S. Heydenreich[1], A. Leauthaud[1], J. DeRose[2]

[1] Department of Astronomy and Astrophysics, UCO/Lick Observatory, University of California, 1156 High Street, Santa Cruz, CA 95064, USA
[2] Physics Department, Brookhaven National Laboratory, Upton, NY 11973, USA

Version July 9, 2025; received xxx, accepted yyy

ABSTRACT

We investigate the impact of a DESI motivated dynamic dark energy cosmology on three cosmological anomalies, the S_8 tension, the 'lensing is low' effect, and observations of strong baryonic feedback. We analyze how these observations vary in ΛCDM versus dynamic dark energy. We find that the galaxy-galaxy lensing signal is reduced by up to 7% with respect to galaxy clustering and that cosmic shear is suppressed by 14%. These differences are primarily caused by changes to cosmological distance measures which enter the lensing efficiency kernels. In contrast, we find that dynamic dark energy increases the thermal Sunyaev Zeldovich signal by about 15%, but that this is insufficient to substantially reduce the magnitude of baryonic effects. Thus, we find that dynamic dark energy may help explain two out of these three cosmological anomalies. DESI's dynamic dark energy has an important impact on cosmic expansion at $z \lesssim 0.5$, a regime where baryon acoustic oscillations are limited by the small volume. Because lensing is sensitive to distances, in addition to growth, we argue that lensing measurements are a promising alternative to constrain expansion deviations from Λ at low redshifts.

Key words. gravitational lensing – weak, cosmology – cosmological parameters, methods – statistical

1. Introduction

The ΛCDM model is resoundingly successful in describing the structure and evolution of the Universe and has rightfully been the cosmological standard model for the last few decades. With the increasing accuracy and precision of cosmological observations, several tensions have emerged (for a review, see Abdalla et al. 2022). While still very actively debated, there appears to be growing evidence that the ΛCDM framework may need to be revised.

In this work, we focus on one potential extension of the ΛCDM model, the w_0w_aCDM model that heuristically allows the equation of state (EoS) of dark energy to vary as a linear function of the scale factor $w = w_0 + w_a(1-a)$.[1] This is particularly motivated by recent analyses of the Dark Energy Spectroscopic Instrument (DESI), which found evidence for evolving dark energy in their flagship analyses of Baryon Acoustic Oscillations (Adame et al. 2025; DESI Collaboration et al. 2024, 2025).[2] Interestingly, allowing for evolving dark energy appears to reduce tensions otherwise present in the constraint on the sum neutrino masses from DESI analyses (Elbers et al. 2025).

In this work, we investigate whether dynamic dark energy can also resolve other tensions present in analyses of the Universe's large-scale structure (LSS), in particular the lack of power present in measurements of the weak gravitational lensing effect. In recent years, analyses of cosmic shear surveys have precisely measured the matter power spectrum, yet these measurements consistently report a value of the matter clustering parameter, $S_8 = \sigma_8 \sqrt{\Omega_\mathrm{m}/0.3}$, that is lower than the one inferred from the cosmic microwave background (Heymans et al. 2021; Dark Energy Survey and Kilo-Degree Survey Collaboration et al. 2023; Amon et al. 2022; Li et al. 2023; Miyatake et al. 2023; Planck Collaboration et al. 2020a). On scales smaller than those typically used for cosmological inference, weak gravitational lensing also appears to yield a lower signal amplitude when compared directly to galaxy clustering measurements, a phenomenon known as the 'lensing is low' effect (Leauthaud et al. 2017; Zu 2020; Lange et al. 2021, 2022, 2023).

It is important to note the possibility that these tensions are merely artifacts of systematic biases or incorrect analysis assumptions. The S_8-tension can be alleviated by allowing a more flexible prescription for the intrinsic alignment of galaxies (Chen et al. 2024), and the most recent analysis by the Kilo-Degree Survey no longer sees a tension in the S_8 parameter (Wright et al. 2025). Likewise, some studies argue that the 'lensing is low' effect is caused by simplistic assumptions in the galaxy-halo connection model (Chaves-Montero et al. 2023; Contreras et al. 2023). In particular, there is a renewed interest in investigating the impact of baryon feedback on lensing observables, as direct observations indicate that this effect is stronger than previously

[1] We note that, while appearing to be a simple Taylor approximation to the 'true' EoS, the choice of parametrization is physically motivated (Chevallier & Polarski 2001; Linder 2003; Scherrer 2015).
[2] In particular, dark energy appears to have been phantom with $w < -1$ at earlier times and only recently crossed the phantom line (Lodha et al. 2025).

assumed (Chen et al. 2023; Terasawa et al. 2025; Bigwood et al. 2024; Hadzhiyska et al. 2024).

In this work, we will investigate whether dynamic dark energy can explain these related tensions, namely the 'lensing is low' effect and the S_8 tension. We will further research whether evidence for excess baryon feedback can also be releated to a preference for dynamic dark energy. This study is particularly motivated by Joudaki et al. (2017), who found that cosmic shear prefers the same type of dynamic dark energy ($w_0 > -1$, $w_a < 0$) that the more recent DESI BAO results seem to favor.

Throughout this work, we will assume the best-fit parameters for the dark energy EoS from the DESI-DR2+CMB+Union3 BAO analysis, namely $w_0 = -0.67$, $w_a = -1.09$, $H_0 = 65.9$, and $\Omega_\mathrm{m} = 0.33$, and investigate how cosmological quantities relate to a ΛCDM cosmology with the same cosmological parameters. We will call the former cosmology the 'DESI-BAO' cosmology, the latter will be denoted by the ΛCDM cosmology.

2. Theoretical background

2.1. Cosmology

We assume a Friedmann-Lemaître-Robertson-Walker metric with curvature $K = 0$ and describe dark energy with the Chevallier-Polarski-Linder parameterization $w(a) = w_0 + w_a(1-a)$ (Linder 2003). Comoving radial distances follow

$$\chi(z) = c\int_0^z \frac{\mathrm{d}z'}{H(z')}\,, \tag{1}$$

where $H^2(z) = H_0^2\big[\Omega_\mathrm{m}(1+z)^3 + \Omega_\mathrm{DE}(z)\big]$ and $\Omega_\mathrm{DE}(z) = \Omega_{\mathrm{DE},0}(1+z)^{3(1+w_0+w_a)}\exp\big[-3w_a z/(1+z)\big]$. Angular diameter distances follow $D_A = \chi/(1+z)$ and enter all projected observables. Linear growth factors $D_+(z)$ are obtained by solving the growth equation with the above $H(z)$ (Hogg 1999). Throughout we use the `Eisenstein & Hu` transfer function (Eisenstein & Hu 1998) and the `HMcode2020` prescriptions for non-linear matter power spectra.

2.2. Galaxy–halo connection

We model the relationship between galaxies and matter with the halo model (Cooray & Sheth 2002). For central and satellite galaxy occupancy we adopt a five-parameter HOD of the form introduced by Zheng et al. (2005), truncated at the virial radius and assuming an NFW density profile for satellites.

2.3. Projected two-point statistics

We model the projected two-point statistics for cosmic shear ($\kappa\kappa$), galaxy-galaxy lensing ($\delta_g\kappa$) and projected clustering ($\delta_g\delta_g$) via their projected power spectra C_ℓ, which can be derived from the 3-dimensional matter power spectrum P via the following relations (e.g. Krause et al. 2017; Limber 1953; Friedrich et al. 2021):

$$\begin{aligned}
C^{ij}_{\kappa\kappa}(\ell) &= \int d\chi \frac{q^i_\kappa(\chi) q^j_\kappa(\chi)}{\chi^2} P\left(\frac{\ell+\frac{1}{2}}{\chi}, z(\chi)\right),\\
C^{ij}_{\delta_g\kappa}(\ell) &= \int d\chi \frac{q^i_\delta\left(\frac{\ell+\frac{1}{2}}{\chi},\chi\right) q^j_\kappa(\chi)}{\chi^2} P\left(\frac{\ell+\frac{1}{2}}{\chi}, z(\chi)\right),\\
C^{ij}_{\delta_g\delta_g}(\ell) &= \int d\chi \frac{q^i_\delta\left(\frac{\ell+\frac{1}{2}}{\chi},\chi\right) q^j_\delta\left(\frac{\ell+\frac{1}{2}}{\chi},\chi\right)}{\chi^2} P\left(\frac{\ell+\frac{1}{2}}{\chi}, z(\chi)\right),
\end{aligned} \tag{2}$$

where i and j denote different combinations for tomographic redshift bins, which we will omit going forward. In the equations above, χ denotes the comoving radial distance, q_κ is the lensing efficiency kernel, and q_δ the radial weight function. They are given by

$$\begin{aligned}
q_\kappa(\chi) &= \frac{3H_0^2\Omega_m\chi}{2a(\chi)}\int_\chi^{\chi_h} d\chi'\left(\frac{\chi'-\chi}{\chi}\right) n_\kappa(z(\chi'))\frac{\mathrm{d}z}{\mathrm{d}\chi'},\\
q_\delta(\chi) &= b\, n_\delta(z(\chi))\frac{\mathrm{d}z}{\mathrm{d}\chi}\,,
\end{aligned} \tag{3}$$

where $n(z)$ denotes the redshift distribution of lenses (for q_δ) and sources (for q_κ), and b is the linear galaxy bias.[3] Configuration-space correlation functions $\xi_\pm(\vartheta)$, γ_t, w_θ are obtained through the methods outlined in Stebbins (1996) and optimized for numerical integration in Friedrich et al. (2021). In our simulation-based analysis, we also utilize the excess surface density $\Delta\Sigma$, which is related to γ_t via (Bartelmann & Schneider 2001)

$$\begin{aligned}
\gamma_\mathrm{t}(\theta) &= \Delta\Sigma\left(\theta\frac{\chi_\mathrm{l}}{(1+z_\mathrm{l})}\right)\Sigma^{-1}_\mathrm{crit}(\chi_\mathrm{l},\chi_\mathrm{s}),\\
\Sigma^{-1}_\mathrm{crit}(\chi_\mathrm{l},\chi_\mathrm{s}) &= \frac{4\pi G}{c^2}\frac{(1+z_\mathrm{l})(\chi_\mathrm{s}-\chi_\mathrm{l})}{\chi_\mathrm{s}}\mathcal{H}(\chi_\mathrm{s}-\chi_\mathrm{l}),
\end{aligned} \tag{4}$$

where $\chi_{\mathrm{l,s}}$ are the comoving radial distances to the lens and source, respectively, and $\mathcal{H}$ is the Heaviside step function.

2.4. Thermal SZ signal and the CAP filter

Thermal Sunyaev-Zeldovich (tSZ) temperature fluctuations are sourced by the Compton-y field, $y \propto \int P_e\,\mathrm{d}l$ (Sunyaev & Zeldovich 1972). We follow Greco et al. (2015) and define the compensated aperture photometry (CAP) filter

$$\begin{aligned}
y_\mathrm{CAP}(\theta) &= \int \mathrm{d}^2\vartheta\, y(\vartheta)\, U_{\theta_\mathrm{ap}}(|\boldsymbol{\vartheta}|),\\
U_{\theta_\mathrm{ap}}(\vartheta) &= \frac{1}{\pi\theta^2_\mathrm{ap}}[\,1-\Theta(\vartheta-\theta_\mathrm{ap})]\\
&\quad - \frac{1}{\pi(\sqrt{2}\,\theta_\mathrm{ap})^2}\Big[\,1-\Theta(\vartheta-\sqrt{2}\,\theta_\mathrm{ap})\Big],
\end{aligned} \tag{5}$$

which removes the large-scale y-mean and facilitates comparison with observations and simulations.

[3] Technically, the galaxy bias is a function of k and z. Here we only compare theoretical predictions between cosmologies; hence, we set b to be constant.

2.5. Used data products

We employ the publicly released lens and source redshift distributions from DESI-DR1 Bright Galaxy Survey (Hahn et al. 2023), DESI-DR1 Luminous Red Galaxies (Zhou et al. 2023), KiDS-1000 (Hildebrandt et al. 2021), DES Year-3 (Myles et al. 2021), and HSC-SSP Year-3 (Rau et al. 2023). All $n(z)$ histograms are re-binned to $\Delta z = 0.005$ and normalised to unity before entering any calculation.

2.6. Used simulations

Non-linear predictions are validated against the AbacusSummit (Maksimova et al. 2021) suite, generated with the high-precision Abacus N-body code (Garrison et al. 2021). We analyse boxes `base_c000_ph000` (ΛCDM) and `base_c111_ph000` (w_0w_aCDM) using the public `TabCorr` package (Neistein et al. 2011; Zheng & Guo 2016; Lange et al. 2019b,a) to tabulate w_p and $\Delta\Sigma$.

3. Methods

We perform two kinds of analyses. Our first approach is a theoretical investigation utilizing the public python library `pyccl`[4] (Chisari et al. 2019). Since we are investigating percent-level effects and power spectrum predictions in dynamic dark energy scenarios are not extensively validated, we supplement this investigation with a simulation-based analysis utilizing `AbacusSummit` and `TabCorr`. While the latter does not provide a perfect match to the DESI best-fit cosmology, it provides a stencil derivative cosmology with the same parameters as the base cosmology, except setting $w_0 = -0.9$ and $w_a = -0.4$. While not close to the best-fit DESI cosmology, it deviates from ΛCDM in the same direction as the DESI best-fit w_0w_aCDM results. We can thus test whether we qualitatively recover the same trends as in the theoretical investigation when comparing this simulation to the base, ΛCDM one.

3.1. Theoretical investigation

We assume the best-fit values of the DESI w_0w_aCDM cosmology ($w_0 = -0.64$, $w_a = -1.27$) and compare different cosmological quantities and observables between this and a fiducial ΛCDM cosmology with the same cosmological parameters.

As a first step, we investigate how dynamic dark energy impacts the individual components that source the final cosmological observables. All LSS observables are impacted by the growth factor, which describes the linear growth of structure and parametrizes the scale-independent evolution of the matter power spectrum over cosmic time. Further, distance measures are also impacted by the Universe's expansion history. They enter all LSS calculations when one converts between angular and phyiscial distances of configuration-space statistics. Crucially, for weak lensing, they additionally enter the calcultions in prefactors quantifying the lensing efficiency q_κ.

Our next step is to compute the projected angular power spectra C_ℓ for quantities of interest, here galaxy clustering, galaxy-galaxy lensing, cosmic shear, and tSZ. We assume a linear bias of $b = 1$ for all tracers for simplicity. We subsequently predict the projected galaxy clustering correlation function w_θ, the tangential shear around galaxies γ_t, and the cosmic shear 2-point correlation functions $\xi_\pm$. We use public redshift distributions of DES-Y3, KiDS, and HSC-Y3 for the source galaxy populations. We further transform the projected tSZ power spectrum into predictions for the compensated aperture (CAP) filter, as used in Hadzhiyska et al. (2024) and other works. For the lens galaxies, we utilize the redshift distributions of DESI-DR1 BGS and LRG.

We then use a matched filter approach, as detailed in Leauthaud et al. (2022) to project the predictions from the DESI-BAO cosmology into a single amplitude, where we take the ΛCDM prediction as the reference data vector and use a covariance for the respective lens-source bin combination as detailed in Yuan et al. (2024). For all purposes, we assume number densities and redshift distributions for the sample of lens galaxies described in Heydenreich et al. (2025). We then compare the amplitude of the different signals in the DESI-BAO cosmology to compare how a deviation from Λ impacts different LSS tracers respectively.

3.2. Simulation-based analysis

The theoretical investigation detailed above faces the caveat that codes modeling nonlinear structure formation have not been extensively validated for non-ΛCDM cosmologies. We thus supplement our analysis by an investigation of the `AbacusSummit` simulation suite, which provides a simulation that deviates from the base cosmology by setting $w_0 = -0.9$ and $w_a = -0.4$. While far away from the DESI best-fit cosmology, the deviation from ΛCDM is in a similar direction as the DESI best-fit w_0w_aCDM results, so we can test whether we qualitatively recover the same trends as in the theoretical investigation when comparing this simulation to the base, ΛCDM one.

We tabulate the projected correlation function w_p and the excess surface density $\Delta\Sigma$, which are related to the w_θ and γ_t statistics above, using the public `TabCorr` code. We then fit an HOD (Zheng et al. 2005) to an observed w_p clustering signal from Leauthaud et al. (2017) using the `nautilus` sampler (Lange 2024), and optimize the fit by performing a scalar minimization of the likelihood at the best-fit cosmology determined by `nautilus`. Using these best-fit HOD parameters, both for the ΛCDM and DESI-BAO cosmology, we then predict the projected clustering w_p (to check consistency) and the excess surface density $\Delta\Sigma$. To compare absolute values, we again use the matched filter approach to compress the DESI-BAO predictions into a single amplitude, given the ΛCDM predictions as the reference data vector.

4. Results

4.1. Cosmological quantities

Dynamic dark energy changes the expansion history of the Universe, and thus impacts both growth factors and distance measures. It is therefore plausible that the conversion from angular to physical coordinates, under the assumption of ΛCDM, could induce biases. As can be seen in Fig. 1, the effect caps at about 3% for $z \sim 0.8$. While certainly relevant for precision cosmology, physical distances differing by 3% alone is unlikely to explain the effects seen in

[4] https://github.com/LSSTDESC/CCL

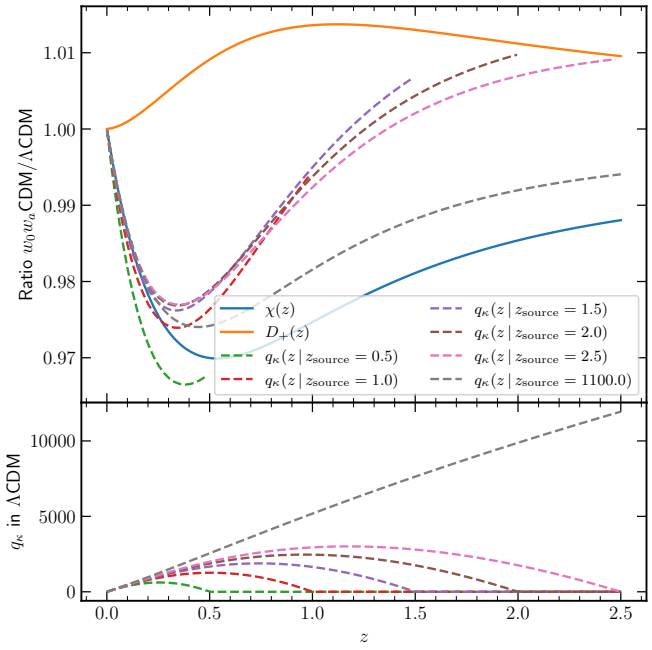

Fig. 1: Top: Ratio of cosmological distances (blue), the normalized growth factor (orange), and lensing efficiencies (dashed lines) under a DESI-BAO model, normalized by the values in the corresponding ΛCDM model. Bottom: The lensing efficiencies q_κ for different source redshifts in ΛCDM.

Leauthaud et al. (2017); Lange et al. (2021, 2022) or in Hadzhiyska et al. (2024). We can see in the same figure that the growth factor is about 1.5% larger at $z \sim 1$ in the DESI-BAO cosmology compared to ΛCDM. Crucially, we find that the lensing efficiency q_κ drops by about 2.5% at $z \sim 0.4$. As this factor does not contribute to clustering observables, but contributes to galaxy-galaxy lensing observables and, squared, to cosmic shear observables, we expect a relative suppression of these statistics with respect to clustering observations.

4.2. Impacts on observables: Theoretical investigation

Dynamic dark energy impacts structure formation in a non-trivial way. We assess the ratio of C_ℓ for projected quantities of interest, here galaxy clustering, galaxy-galaxy lensing, cosmic shear, and tSZ.

As a first investigation, we estimate the impact of a DESI-BAO cosmology by predicting projected angular power spectra for galaxy clustering, galaxy-galaxy lensing, cosmic shear, tSZ, and CMB lensing. To simplify our assumptions, we model the redshift distributions as Gaussians of width $\sigma = 0.2$; the lens redshifts are centered around $z \in \{0.2, 0.3, 0.4, 0.5\}$, the source redshifts vary between $0.3 \leq z \leq 1.5$. We then compare the ratio of the C_ℓ for the DESI-BAO cosmology to the ΛCDM cosmology in Fig. 2. We can observe a few general trends:

- Projected galaxy clustering is increased in the DESI-BAO cosmology. The amount of increase increases with redshift from 5% at $z = 0.2$ to 10% at $z = 0.5$. This is caused both by the increase in the growth factor D_+, and by a decrease in the comoving distance χ, which increases $\mathrm{d}z/\mathrm{d}\chi$ in q_δ (Eq. 3).
- Galaxy-galaxy lensing increases with both source- and lens-redshift in the DESI-BAO cosmology with respect to ΛCDM. For low source- and lens-redshift we observe a slight decrease of the GGL signal, whereas for high lens- and source-redshifts the ratio is slightly above unity. Here, the increase in the growth factor gets countered by a general decrease of q_κ. This is most effective when the lens galaxy populations are in the region where q_κ is suppressed most ($z \sim 0.35$). With increasing source redshift, the suppression of q_κ decreases, and the region where q_κ is suppressed the most no longer strongly contributes to the lensing signal, as the absolute value of q_κ around $z \sim 0.35$ becomes very small.
- Cosmic shear is decreased in the DESI-BAO cosmology by about 12% for low source redshifts and a few per-cent for high source redshifts. The decrease of cosmic shear is stronger than for GGL, as q_κ enters the equation twice. The amount of signal suppression depends both on the amount that q_κ drops, as well as on the value of q_κ around that drop. For high source redshifts, the region around $z \sim 0.35$ does not contribute substantially to the lensing signal, meaning that the lower lensing efficiency at these redshifts is no longer as relevant.
- The CMB lensing signal is relatively unaffected by the change in cosmology. While the q_κ drops strongly for the CMB lensing signal, the CMB lensing efficiency is practically negligible at $z < 0.5$, meaning that this drop does not substantially impact the lensing signal, and gets counter-acted by the increased growth rate.
- The excess in tSZ signal increases with lens redshift, from about 10% at $z = 0.2$ to 15% at $z = 0.5$. This is likely sourced by the non-linear relationship between halo mass (which in turn relates to the growth factor) and tSZ signal, with tSZ $\propto M^{\frac{5}{3}}$.

Overall, we see that summary statistics in the DESI-BAO cosmology behave in a way that is consistent with the observed 'lensing is low' trend – the GGL signal is suppressed by 5%-15% with respect to the galaxy clustering, depending on source and lens redshift, and the cosmic shear signal is suppressed by up to 30% with respect to galaxy clustering. This could explain both a lower S_8 value measured by cosmic shear surveys and the more direct lensing is low effect, which describes a lack of power of the GGL signal with respect to galaxy clustering.

Regarding excess baryon feedback, the conclusion is a bit less unanimous. While we do predict an increased tSZ signal around galaxies by about 15% in the DESI-BAO cosmology, this is not necessarily equivalent to an extended baryon feedback scenario. As can be seen in Hadzhiyska et al. (2024), at least in the kSZ, the extended baryon feedback signal manifests in a decrease of the signal at smaller scales, where the baryons are expelled from the halo.

We note that DESI shows a large degeneracy along the w_0-w_a axis, so that stronger deviations from ΛCDM, and thus also a stronger suppression of GGL and cosmic shear with respect to galaxy clustering, are definitely plausible.

4.3. A realistic case: Configuration space statistics with DESI x HSC, KiDS, DES and ACT

Instead of general redshift trends, we now investigate a realistic scenario of GGL and projected clustering measure-

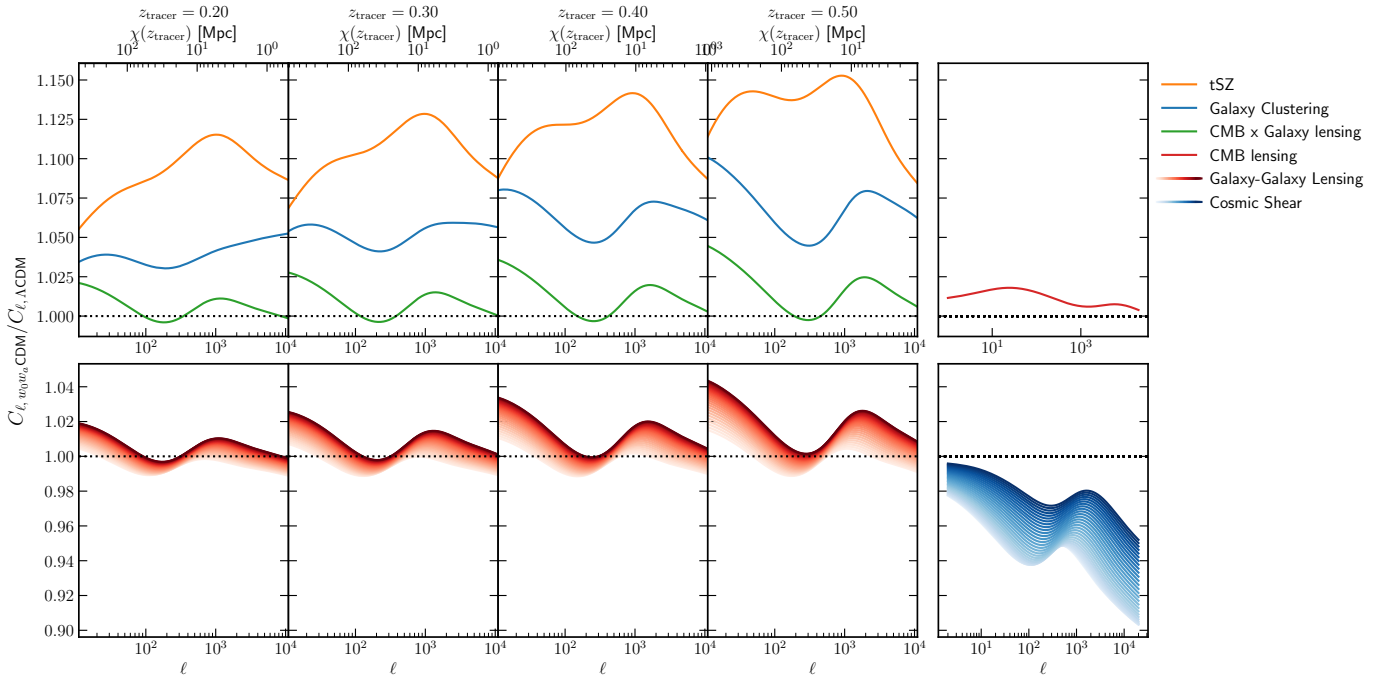

Fig. 2: Ratio of projected angular power spectra C_ℓ under a DESI-BAO cosmology vs a ΛCDM cosmology. The left four columns represent different redshifts of tracer galaxy populations. The right-most column shows quantities that do not depend on tracer populations (CMB lensing and cosmic shear). The top row shows the tSZ, galaxy clustering, and CMB x Galaxy lensing signal ratios for the tracer galaxy populations in the left columns, and the CMB lensing signal ratio in the right column. The bottom row on the left shows the galaxy-galaxy lensing signal ratio for different source redshifts, where the tracer galaxy population constitutes the lens galaxies. On the right, we show the cosmic shear signal ratio. The color coding for the galaxy-galaxy lensing and cosmic shear signals indicates source redshift distributions varying between $z = 0.3$ (light colors) and $z = 1.5$ (dark colors).

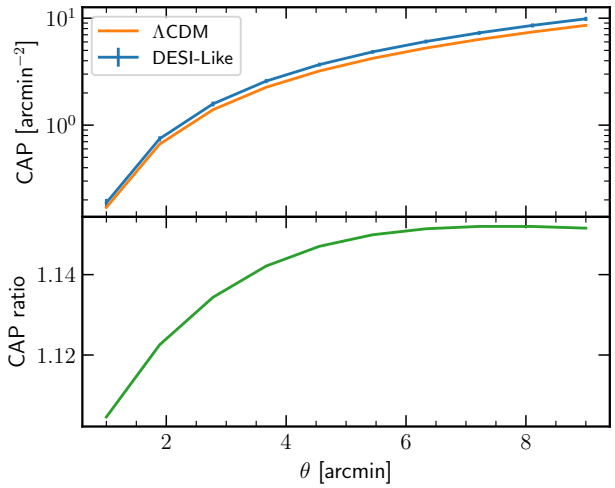

Fig. 3: Projected tSZ signal around galaxies in a DESI-BAO cosmology compared to ΛCDM using the more commonly used compensated aperture filter (CAP) technique. While the total tSZ signal increase is 15%, strong baryon feedback is characterized by a signal drop on small scales relative to the large scales. This drop is present, but observed baryonic effects are much larger.

ments using DESI-DR1 lens galaxies and source galaxies from the three major Stage-III lensing surveys. As above, we compare the predictions of CCL in the DESI-BAO cosmology and ΛCDM. We utilize the redshift distributions of the measured tracers and transform the predicted power spectra to their configuration space equivalents. To better compare measurements, we project the DESI-BAO predictions to a single amplitude using the matched filter approach, where we take covariance estimates computed as in Yuan et al. (2024), and the reference data vector is the ΛCDM prediction. In Fig. 4 we show the results for cross-correlations between DESI and HSC-Y3. A clear picture emerges, which confirms the theoretical investigations above: The GGL signal is suppressed, with respect to the projected clustering signal, by up to 7%, where the suppression is largest for small lens-source separations. The cosmic shear signal is suppressed by up to 13% with respect to the projected clustering signal, where the suppression is strongest for high lens and small source redshifts. Interestingly, the fact that this suppression increases when the lens-source distance decreases, implies that an effect like this can potentially be masked by an uninformative intrinsic alignment model.

4.4. Simulation-based analysis

To validate our theoretical investigations, we perform a simulation-based analysis by comparing $\Delta\Sigma$ signals between a ΛCDM and a DESI-BAO-like cosmology, where the

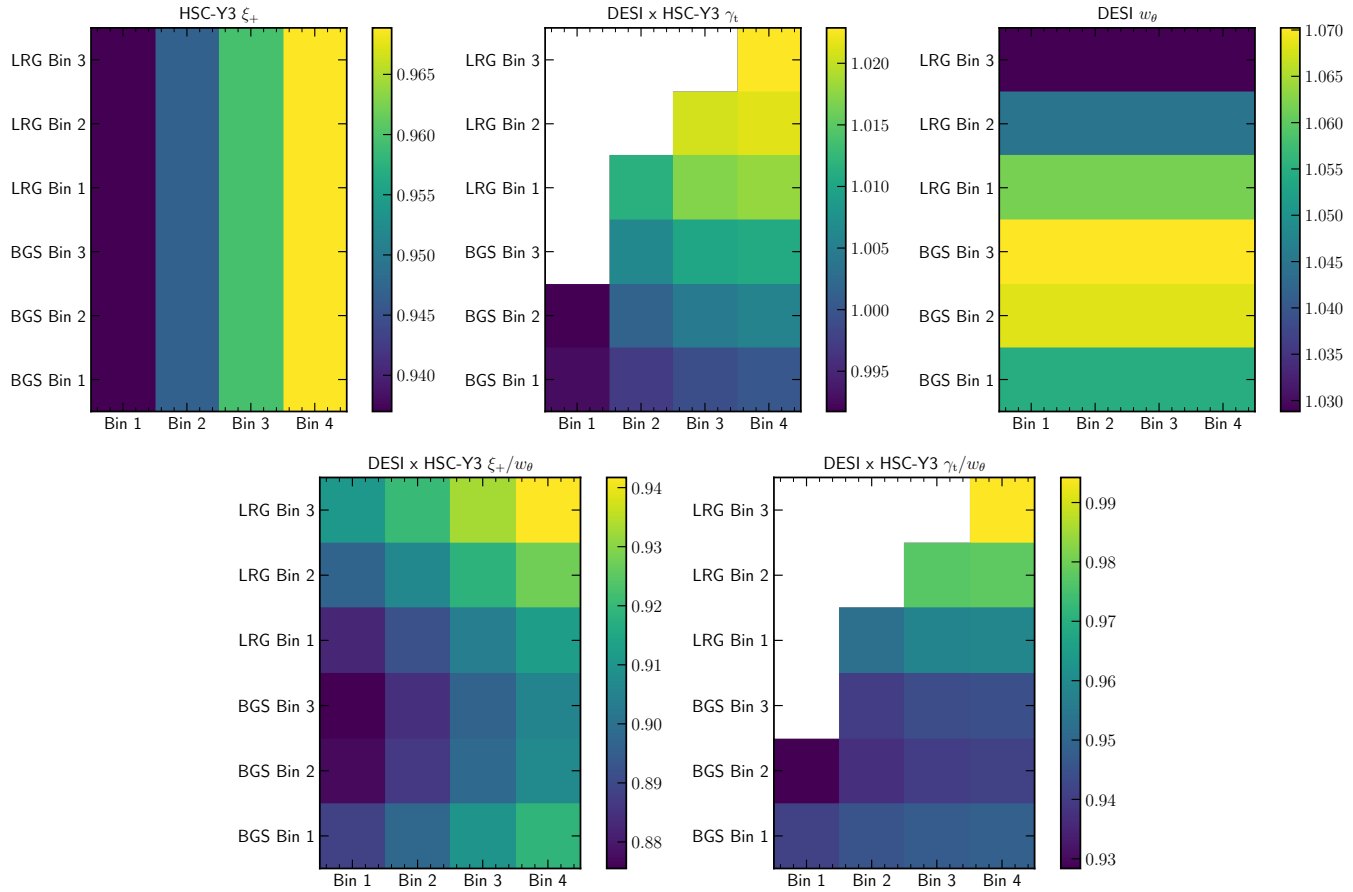

Fig. 4: Top row: Predicted amplitudes of projected clustering, tangential shear, and cosmic shear in the DESI-BAO cosmology compared to ΛCDM for DESI-DR1 lenses and HSC-Y3 source galaxies. Bottom row: Ratios of the lensing to clustering amplitudes in the DESI-BAO cosmology divided by the same ratios in ΛCDM.

HODs that model the $\Delta\Sigma$ signals are fitted to the observed projected clustering signal.

We find that the predicted projected clustering signals are consistent between ΛCDM and the DESI-BAO cosmology, with the DESI-BAO prediction showing an amplitude of 0.998. As the HODs were explicitly tuned to achieve consistent clustering, this is not surprising at all, but serves as an important validation check to confirm that fitting accuracy and flexibility do not impact our results. In contrast, the excess surface density shows a 2% decrease, exhibiting an amplitude of 0.978. While not a strong effect, linearly extrapolating this to the best-fit cosmology of the DESI-DR2 analysis, it matches with the predictions from the theoretical investigations above, making a strong case for their validity.

5. Discussion

5.1. Dynamic dark energy and the lensing is low effect

The lensing is low effect describes a discrepancy between the amplitude of the projected clustering signal and the GGL signal. This discrepancy is most pronounced in the KiDS survey, where the GGL signal is about 15% lower than expected from the projected clustering signal. A dynamic dark energy scenario at the best-fit cosmology of DESI-DR1 would account for about half of that discrepancy, as we observe an up to 10% suppression of the GGL signal. As an additional benefit, the S_8 tension would also be alleviated, as the cosmic shear signal is suppressed by 10% to 15% with respect to the projected clustering signal. While the DESI-DR1 best-fit result can not fully account for the lensing is low effect, DESI shows a strong degeneracy along the w_0-w_a axis, so that stronger deviations from ΛCDM are definitely plausible, and both the lensing is low effect and the S_8 tension can potentially be alleviated by allowing for dynamic dark energy. Further studies combining DESI's BAO measurements with studies of Galaxy-Galaxy lensing and cosmic shear will be able to provide powerful constraints on the w_0-w_a plane, potentially breaking the degeneracy present in current BAO and RSD measurements.

We further identify that the main impact of dynamic dark energy on lensing observables is not from a different growth factor of the power spectrum. Instead, the difference stems from changes in the lensing efficiency prefactors, $\Delta\Sigma$ and q_κ, which are sensitive to changes in the distance-redshift relation. This is important to keep in mind e.g. when investigating Fig. 6 of (DESI Collaboration et al. 2024), which shows that the posteriors of S_8 do not change between ΛCDM and w_0w_aCDM in the DESI full-shape analysis of the galaxy power spectrum. From this, one might be tempted to conclude that the S_8 tension can not be sourced from this difference. However, this neglects the differences of how the lensing observables relate to the matter powerspectrum outlined above. When these are taken into

account, dynamic dark energy with $w_0 > -1$ and $w_a < 0$ is a promising model to resolve the lensing is low effect and the S_8 tension.

The latter insight is particularly crucial when one wants to analyze tensions in structure growth measurements in the presence of dynamic dark energy. Fig. 1 of Sailer et al. (2025) compares changes in growth factor and distances for the Planck Collaboration et al. (2020a) best-fit ΛCDM cosmology with both the DESI best-fit ΛCDM cosmology and the DESI BAO cosmology. One can see that the differences in growth are highly degenerate, whereas the functional form of the changes to distances (and hence lensing efficiencies) differs. Considering that this change dominates at low redshifts, where direct distance measurements via BAOs at $\sim 100\,\mathrm{Mpc}/h$ are limited by a small volume, **a combined analysis of lensing and clustering offers the best way to determine whether growth tensions can be attributed to a departure from Λ.**

5.2. Caveats

This work constitutes an exploratory investigation of the potential of a w_0w_aCDM cosmology to resolve the lensing is low effect and the evidence for strong baryon feedback. We do not claim to have performed a full analysis of these two effects, but rather to investigate if dynamical DE has the potential to "solve" these two cases in one fell swoop. We find that this is indeed the case for the lensing is low effect and find some interesting trends regarding baryon feedback, but we also note that there are several caveats to this work:

- pyccl does not model the kinetic Sunyaev Zeldovich effect. The tSZ ($\propto M^{5/3}$) has a different mass dependence than kSZ ($\propto M$). Impacts on kSZ are thus so far hard to predict.
- Deviations from ΛCDM are coupled to shifts in other cosmological parameters in the DESI results. Comparisons to a ΛCDM cosmology with the same parameters is thus not necessarily a fair representation of a true cosmological parameter inference. We refer the reader again to Fig. 1 of Sailer et al. (2025) to see how departures from Λ impact growth and distance compared to changes in cosmlogical parameters within ΛCDM.

While further work is certainly needed, this exploratory study serves to further motivate a rigorous investigation of dynamic dark energy models using a combination of lensing and clustering data.

Acknowledgements

We are thankful to Chris Blake for making his covariance calculations available to us. SH is supported by the U.D Department of Energy, Office of Science, Office of High Energy Physics under Award Number DE-SC0019301.

References

Abdalla, E., Abellán, G. F., Aboubrahim, A., et al. 2022, Journal of High Energy Astrophysics, 34, 49
Adame, A. G., Aguilar, J., Ahlen, S., et al. 2025, J. Cosmology Astropart. Phys., 2025, 021
Amon, A., Gruen, D., Troxel, M. A., et al. 2022, Phys. Rev. D, 105, 023514
Bartelmann, M. & Schneider, P. 2001, Phys. Rep., 340, 291
Bigwood, L., Amon, A., Schneider, A., et al. 2024, MNRAS, 534, 655
Chaves-Montero, J., Angulo, R. E., & Contreras, S. 2023, MNRAS, 521, 937
Chen, A., Aricò, G., Huterer, D., et al. 2023, MNRAS, 518, 5340
Chen, S., DeRose, J., Zhou, R., et al. 2024, Phys. Rev. D, 110, 103518
Chevallier, M. & Polarski, D. 2001, International Journal of Modern Physics D, 10, 213
Chisari, N. E., Alonso, D., Krause, E., et al. 2019, ApJS, 242, 2
Contreras, S., Chaves-Montero, J., & Angulo, R. E. 2023, MNRAS, 525, 3149
Cooray, A. & Sheth, R. 2002, Phys. Rep., 372, 1
Dark Energy Survey and Kilo-Degree Survey Collaboration, Abbott, T. M. C., Aguena, M., et al. 2023, The Open Journal of Astrophysics, 6, 36
DESI Collaboration, Abdul-Karim, M., Aguilar, J., et al. 2025, arXiv e-prints, arXiv:2503.14738
DESI Collaboration, Adame, A. G., Aguilar, J., et al. 2024, arXiv e-prints, arXiv:2411.12022
Eisenstein, D. J. & Hu, W. 1998, ApJ, 496, 605
Elbers, W., Aviles, A., Noriega, H. E., et al. 2025, arXiv e-prints, arXiv:2503.14744
Friedrich, O., Andrade-Oliveira, F., Camacho, H., et al. 2021, MNRAS, 508, 3125
Garrison, L. H., Eisenstein, D. J., Ferrer, D., Maksimova, N. A., & Pinto, P. A. 2021, MNRAS, 508, 575
Greco, J. P., Hill, J. C., Spergel, D. N., & Battaglia, N. 2015, ApJ, 808, 151
Hadzhiyska, B., Ferraro, S., Ried Guachalla, B., et al. 2024, arXiv e-prints, arXiv:2407.07152
Hahn, C., Wilson, M. J., Ruiz-Macias, O., et al. 2023, AJ, 165, 253
Heydenreich, S., Leauthaud, A., Blake, C., et al. 2025, arXiv e-prints, arXiv:2506.21677
Heymans, C., Tröster, T., Asgari, M., et al. 2021, A&A, 646, A140
Hildebrandt, H., van den Busch, J. L., Wright, A. H., et al. 2021, A&A, 647, A124
Hogg, D. W. 1999, arXiv e-prints, astro
Joudaki, S., Mead, A., Blake, C., et al. 2017, MNRAS, 471, 1259
Krause, E., Eifler, T. F., Zuntz, J., et al. 2017, arXiv e-prints, arXiv:1706.09359
Lange, J. U. 2024, in American Astronomical Society Meeting Abstracts, Vol. 244, American Astronomical Society Meeting Abstracts, 229.02
Lange, J. U., Hearin, A. P., Leauthaud, A., et al. 2022, MNRAS, 509, 1779
Lange, J. U., Hearin, A. P., Leauthaud, A., et al. 2023, MNRAS, 520, 5373
Lange, J. U., Leauthaud, A., Singh, S., et al. 2021, MNRAS, 502, 2074
Lange, J. U., van den Bosch, F. C., Zentner, A. R., et al. 2019a, MNRAS, 490, 1870
Lange, J. U., Yang, X., Guo, H., Luo, W., & van den Bosch, F. C. 2019b, MNRAS, 488, 5771
Leauthaud, A., Amon, A., Singh, S., et al. 2022, MNRAS, 510, 6150
Leauthaud, A., Saito, S., Hilbert, S., et al. 2017, MNRAS, 467, 3024
Li, X., Zhang, T., Sugiyama, S., et al. 2023, Phys. Rev. D, 108, 123518
Limber, D. N. 1953, ApJ, 117, 134
Linder, E. V. 2003, Phys. Rev. Lett., 90, 091301
Lodha, K., Calderon, R., Matthewson, W. L., et al. 2025, arXiv e-prints, arXiv:2503.14743
Maksimova, N. A., Garrison, L. H., Eisenstein, D. J., et al. 2021, MNRAS, 508, 4017
Miyatake, H., Sugiyama, S., Takada, M., et al. 2023, Phys. Rev. D, 108, 123517
Myles, J., Alarcon, A., Amon, A., et al. 2021, MNRAS, 505, 4249
Neistein, E., Li, C., Khochfar, S., et al. 2011, MNRAS, 416, 1486
Planck Collaboration, Aghanim, N., Akrami, Y., et al. 2020a, A&A, 641, A6
Planck Collaboration, Aghanim, N., Akrami, Y., et al. 2020b, A&A, 641, A6
Rau, M. M., Dalal, R., Zhang, T., et al. 2023, MNRAS, 524, 5109
Sailer, N., DeRose, J., Ferraro, S., et al. 2025, Phys. Rev. D, 111, 103540
Scherrer, R. J. 2015, Phys. Rev. D, 92, 043001
Stebbins, A. 1996, arXiv e-prints, astro
Sunyaev, R. A. & Zeldovich, Y. B. 1972, Comments on Astrophysics and Space Physics, 4, 173
Terasawa, R., Li, X., Takada, M., et al. 2025, Phys. Rev. D, 111, 063509
Wright, A. H., Stölzner, B., Asgari, M., et al. 2025, arXiv e-prints, arXiv:2503.19441
Yuan, S., Zhang, H., Ross, A. J., et al. 2024, MNRAS, 530, 947
Zheng, Z., Berlind, A. A., Weinberg, D. H., et al. 2005, ApJ, 633, 791
Zheng, Z. & Guo, H. 2016, MNRAS, 458, 4015
Zhou, R., Dey, B., Newman, J. A., et al. 2023, AJ, 165, 58
Zu, Y. 2020, arXiv e-prints, arXiv:2010.01143